Journal of Cerebral Blood Flow & Metabolism (2012) 32, 1000–1013

www.jcbfm.com

A nonlinear dynamical theory of cell injury

Donald J DeGracia[1], Zhi-Feng Huang[2] and Sui Huang[3]

[1]*Department of Physiology, Wayne State University, Detroit, Michigan, USA;* [2]*Department of Physics and Astronomy, Wayne State University, Detroit, Michigan, USA;* [3]*Institute of Systems Biology, Seattle, Washington, USA*

Multifactorial injuries, such as ischemia, trauma, etc., have proven stubbornly elusive to clinical therapeutics, in spite of the binary outcome of recovery or death. This may be due, in part, to the lack of formal approaches to cell injury. We present a minimal system of nonlinear ordinary differential equations describing a theory of cell injury dynamics. A mutual antagonism between injury-driven total damage and total induced stress responses gives rise to attractors representing recovery or death. Solving across a range of injury magnitudes defines an 'injury course' containing a well-defined tipping point between recovery and death. Via the model, therapeutics is the diverting of a system on a pro-death trajectory to a pro-survival trajectory on bistable phase planes. The model plausibly explains why laboratory-based therapies have tended to fail clinically. A survival outcome is easy to achieve when lethal injury is close to the tipping point, but becomes progressively difficult as injury magnitudes increase, and there is an upper limit to salvageable injuries. The model offers novel insights into cell injury that may assist in overcoming barriers that have prevented development of clinically effective therapies for multifactorial conditions, as exemplified by brain ischemia.
Journal of Cerebral Blood Flow & Metabolism (2012) **32,** 1000–1013; doi:10.1038/jcbfm.2012.10; published online 7 March 2012

Keywords: bistability; brain ischemia; cell injury; nonlinear dynamics; therapeutics

Introduction

Over 1,000 agents have shown neuroprotection in preclinical animal studies of brain ischemia, but over 100 of these agents taken to stroke neuroprotection clinical trials have failed (O'Collins *et al*, 2006). Even the guidelines of the Stroke Treatment Academic Industry Roundtable (STAIR) group could not prevent clinical trial failure in the face of stringent preclinical protocols (Savitz, 2007; Philip *et al*, 2009). Thus, the field is faced with an enormous paradox: almost 'anything' can serve as a neuroprotectant in experimental animals, but no pharmacological treatment has thus far translated to human neuroprotection. We offer here an alternative view of cellular injury that, among other things, offers a plausible explanation for this neuroprotection paradox.

O'Collins *et al* (2006) suggested that the problem might not be technical, but theoretical, and that alternative ways to think about ischemic brain injury may be required. The currently dominant paradigm driving the field is the 'ischemic cascade,' a detailed description of the molecular pathways induced in brain cells by ischemia. The term 'cascade' implies a linear sequence of cause and effect. But on-going research has revealed so many changes in neuronal molecular biology that it is difficult to maintain these occur in a sequential manner, making the notion that ischemia induces a molecular cascade increasingly threadbare. We recently suggested that systems biology concepts may provide an alternative framework for understanding neuronal ischemic injury. In DeGracia (2010*a*, *b*, *c*, *d*), existing data were interpreted to indicate that ischemia induces a nonlinear, intracellular influence network of pro-survival and pro-death changes, the mutual antagonism of which causes outcome.

Here, we take the next step and present a dynamical mathematical model, implementing the concepts in DeGracia (2010*a*, *b*, *c*, *d*), that describes how total damage and total stress responses change in time as a function of injury magnitude. Although motivated by the findings in brain ischemia, this model is not specifically about ischemia. Because it describes the mathematical relationship between total damage, total induced stress responses, and injury magnitude, it can be taken as a general model of cellular injury, or be considered a 'toy model.' The

Correspondence: Dr DJ DeGracia, Department of Physiology, Wayne State University, 4116 Scott Hall, 540 East Canfield Avenue, Detroit, MI 48201, USA.
E-mail: ddegraci@med.wayne.edu
This work was supported by NINDS NS 057167 (DJD) and by NSF DMR-0845264 (Z-FH). SH is Alberta Innovates the Future (AITF) Scholar.
Received 25 January 2012; accepted 25 January 2012; published online 7 March 2012

term 'toy model' is not derogatory, but is commonly used in physical sciences to facilitate the exploration of general principles that could be valid for an entire class of systems. The simplification afforded by a toy model is often needed to expose elementary principles that, unobstructed by idiosyncratic details, the human mind readily comprehends (Picht, 1969). If our simplified but formal model system indeed sheds useful light on known features of cell injury that have resisted traditional qualitative explanation, this will corroborate the reasoning behind the mathematical model.

The model provides a critical systematic and quantitative overlay to what is otherwise a list of qualitative and idiosyncratic biological details pertaining to injured cells. In addition, studying the model expands the scope of inquiries into cell injury to encompass concepts routinely and successfully applied in physics and engineering to describe the behavior of complex systems, which increasingly apply to a diversity of complex biological systems (Tyson *et al*, 2001; Huang and Wikswo, 2006).

The paper contains three parts. In part 1, we construct a 'minimal model,' or the simplest mathematical form that captures dynamics resembling real cell injury. Part 2 discusses solution output of the model, focusing on the novel concept of an *injury course*: the time courses of total damage and total stress responses across all relevant injury magnitudes. The injury course appears a natural way to describe cellular injury, ischemic, or otherwise. Part 3 links the model to therapy. Armed with the new conceptual tools, therapy can be more tangibly described as the shifting of an injured system on a pro-death trajectory to a pro-survival trajectory. When the system possesses bistable dynamics, therapy can be achieved by altering the initial conditions of the system. We find that increasingly lethal injury magnitudes in bistable phase planes require progressive increases in initial conditions to convert a pro-death state to a survival state. This provides a plausible explanation for why so many agents act as laboratory neuroprotectants, but fail in clinical trials.

Part I: Building the model

Point of Departure

It is well established that brain I/R (ischemia and reperfusion) injury is multifactorial; that is, it induces many cellular damage mechanisms (Lipton, 1999; Hossmann, 2009). The Wieloch 'sandwich model' (Dirnagl and Meisel, 2008) provides a seminal framework to understand how these integrate to generate outcome. The sandwich model stacks individual damage mechanism, where the height represents each damage mechanism's intensity (Figure 1). The total height of this 'sandwich' is then the total amount of damage (D_T) experienced by the cell. The model posits a threshold amount of damage (D_{TH}), below which the cell survives, and above which it dies. It offers two seminal concepts: (1) the cause of cell death can be defined mathematically: if $D_T > D_{TH}$, the cell dies and (2) the outcome is caused by the aggregate effect of all injury-induced damage.

Expanding the Sandwich Model

In addition to damaging cells, the brain I/R causes cells to induce intrinsic protective mechanisms we generically refer to as 'stress responses.' By analogy, we stack individual stress responses to obtain 'total induced stress responses,' S_T (Figure 1). Then, the threshold amount of damage (D_{TH}) the cell can withstand can be linked to stress response induction: the higher S_T, the higher will be D_{TH}. Thus, the sandwich model implies stress response induction. This expanded sandwich model provides the following core premises for constructing a formal model of cell injury:

1. The cause of cell death can be approached mathematically.
2. We must consider the aggregate effect of all damage mechanisms (D_T) and all stress responses (S_T).
3. D_T and S_T interact to determine outcome.

Developing a Formal Model of Cell Injury

Building on the above premises, coupled with analytical techniques now standard in systems biology (Kaplan and Glass, 1995; Alon, 2006), we construct our toy model of cell injury, embodied as a system of nonlinear ordinary differential equations (ODEs). Before introducing the mathematical form, we elaborate the qualitative picture that we wish to represent mathematically.

Domain of the Model

The model describes a single injured cell. This cell has two features: (1) its phenotype and (2) the complex molecular events occurring within it. The latter is treated as a 'black box' because we are unconcerned with the specific biological details. The cell phenotype is taken as a manifestation of the global dynamics of the underlying intracellular events. The latter are constrained and channeled by gene regulatory networks that produce coherent cell behaviors, including discrete, binary fate decisions (Huang, 2009, 2011). For cell injury, the relevant binary phenotypic decision is survival or death. Thus, as described below, the intracellular events are binned and treated in aggregate as either pro-survival or pro-death.

That we consider only a single injured cell may seem too restrictive because tissue and organ injury is the focus of clinical interest. However, tissues and organs are made of cells that contain identical

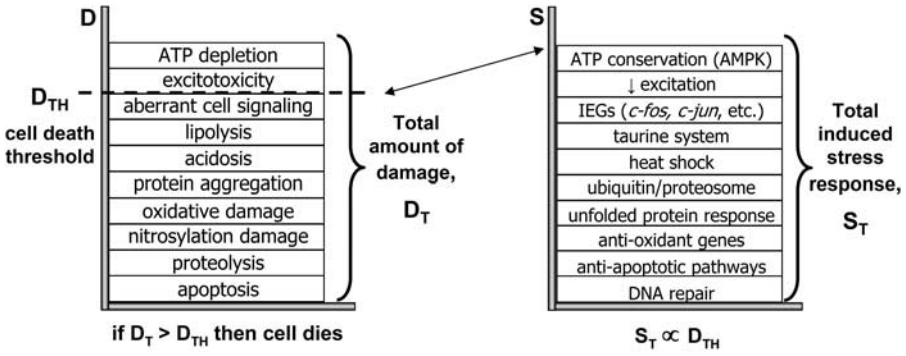

Figure 1 (Left) The Wieloch sandwich model illustrated using damage mechanisms known to be induced in neurons following brain ischemia and reperfusion. The list is meant to be representative not exhaustive. (Right) The Wieloch sandwich model expanded to include stress responses. The list of stress responses also draws on those known to be induced in neurons and is representative not exhaustive. AMPK, adenosine monophosphate-activated protein kinase; IEG, immediate early gene. The arrow between the boxes indicates that the height of total induced stress responses (S_T) effectively sets the cell death threshold (D_{TH}), or the amount of total damage the cell can withstand and thus survive.

molecular biological apparatus and often act in chorus such that the behavior of an individual cell, the smallest functional entity that succumbs or recovers following injury, can represent a relevant tissue domain. We envision future models will consider groups of distinct, interacting cells to better represent organs and tissues.

The Conceptual Picture

Our toy model offers sufficient specifics that capture biological observation, yet is simple enough to act as substrate to develop a formal theory of what causes cells to either recover or die after being injured. The qualitative formulation of the theory can be expressed as follows.

When a cell is injured, the injury simultaneously: (1) damages the cell and (2) causes the cell to induce stress responses. The damage and stress responses compete because they are inherently mutually antagonistic. If, at the end of this competition, the remaining total damage is greater than the remaining total stress responses, the cell dies. If the stress responses win out over damage, the cell recovers. Thus, the essence of the theory is that cell death is caused when the total amount of damage, D, exceeds the cell's total induced stress response capacity, S, that is, when $D > S$. What causes this inequality is the magnitude of the injury, I.

Empirically, specific forms of cell damage follow from the nature of the damage agent, the intensity of its application, and the nature of the injured cell, resulting in specific biological details. Our theory of cell death causation is independent of these details. It is a blanket generic statement that an injured cell will die when the total damage exceeds the cell's total induced capacity to combat it.

We now express these ideas mathematically. First, we model the time course of the D–S competition. Then, we incorporate the magnitude of injury, I, as a driver of the magnitudes of D and S.

Mutual Antagonism of D and S

Following Huang *et al* (2007), we can describe the D–S mutual antagonism using the following system of coupled nonlinear ODEs. The mutual inhibition of D and S are modeled as sigmoidal relationships using Hill functions (Supplementary Figure S1):

$$\begin{aligned}\frac{dD}{dt} &= v_D \frac{\Theta_D^{n_D}}{\Theta_D^{n_D} + S^{n_D}} - k_D D \\ \frac{dS}{dt} &= v_S \frac{\Theta_S^{n_S}}{\Theta_S^{n_S} + D^{n_S}} - k_S S\end{aligned} \tag{1}$$

Equation (1) describes the rates of change of the variables D and S. Each ODE has four analogous parameters: v, Θ, n, and k. Taking D and S as equivalents of concentrations, v_D and v_S are velocities in units of concentration $\times$ 1/time. The k_D and k_S are first-order decay constants with units of 1/time. The exponents n_D and n_S are Hill coefficients. Θ_D, the threshold of D, is a specific amount of D that inhibits S by 50%. Θ_S, the threshold of S, inhibits D by 50%.

Equation (1) is well studied in molecular biology and is used to model the action of two mutually inhibitory factors (Huang *et al*, 2007). Each ODE has the same form, consisting of two terms on the right-hand side. The first term is an accumulation term, the second a decay term. The interpretation of equation (1) is straightforward: the rate of change equals the rate of accumulation minus the rate of decay (Alon, 2006).

The accumulation term models the mutual antagonism of D and S by: (1) coupling the two variable's inverse relationships ($dD/dt \propto 1/S$ and $dS/dt \propto 1/D$) and (2) containing the threshold parameters. This

expression is intuitive when interpreted in terms of its physical meaning. For example, a large value for S (compared with D) means the stress responses are strong and will slow the rate of change of damage by inhibiting its formation. Additionally, strong stress responses will have a high threshold against inhibition by damage (Θ_S is large compared with D) so that the ratio $\Theta_S^{n_S}/(\Theta_S^{n_S}+D^{n_S}) \sim \Theta_S^{n_S}/(\Theta_S^{n_S}+0) \sim 1$ and S accumulates approaching its maximum rate, v_S. Opposite logic applies if $D > S$.

The second term on the right-hand side is a first-order decay. Here, it is not unreasonable to assume that the decays of D and S are uncoupled. Generally, damage does not shut-off stress response pathways. Stress response pathways usually fade off when not sustained by the stressor. Similarly, damage is not cleared by molecular pathways that inhibit damage, but is eventually cleared by downstream cellular 'garbage cans' such as proteosomes, lysosomes, or autophagy that are not injury specific.

Incorporating Injury, *I*

Our modifications to equation (1) to incorporate I are novel. Our treatment is therefore guided by minimalist modeling assumptions, made explicit as we proceed.

We first explain injury magnitude, I, by way of example. Imagine a series of 20 rats, numbered 1 to 20. Each rat is given the same minutes of complete global brain ischemia as its number: rat 1 gets 1 minute ischemia, rat 2 gets 2 minutes, and so on. Then, we wish to study (in a well-defined cell population, such as hippocampal CA1) the D and S time courses, determining their peak values in each rat. Intuitively, peak D and S will be low at low injury magnitudes. At intermediate injury values, peak values of D and S will be larger. At high magnitudes of injury, peak D will be larger still, but peak S will be smaller, because damage becomes so strong it prevents the action of the stress responses. Thus, each value of I, exampled here by the minutes of ischemia, is one specific insult that will play out by D and S competing over time, resulting in either recovery or death. Thinking of a range of injury magnitudes, where each value of I displays its own D–S competition, illustrates qualitatively our concept of an *injury course*, which is developed into a precise quantitative concept below.

We posit that I will exponentially drive D and S. The expected patterns of change are captured by the form $y = xe^{x}$ or xe^{-x} (Figure 2). The positive exponent case models the continuous increase in total damage, D, with I. The negative exponent case models how total induced stress responses, S, first increase, then decrease, as I increases.

We model the effect of I on D and S through the parameters in equation (1). In principle, the D and S parameters can change as Ie^{I} or Ie^{-I} as shown in equation (2), where the c's are proportionality

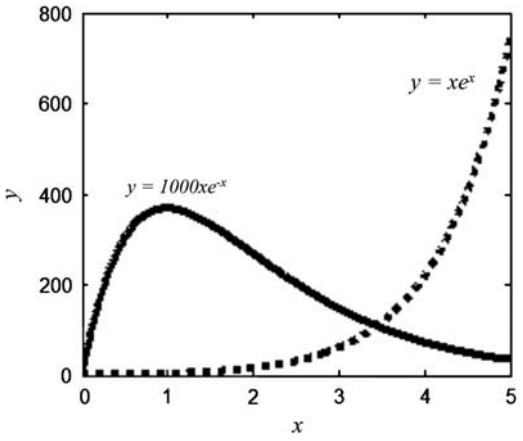

Figure 2 The functional form $y = xe^{x}$. When the exponent is positive (dashed curve), the function increases continuously with x; this is used to model the increase in total damage, D, with injury magnitude, I. When the exponent is negative (solid curve), the function increases for $x < 1$, but decreases for $x > 1$; this form is used to model how total induced stress responses, S, change with I. Since these functions are exponential and change rapidly with x, the negative exponent case is multiplied by 1,000 so that the two curves can be plotted at similar scales.

constants, and the λ's are analogous to time constants:

$$\begin{aligned} v_D &= c_1 I e^{+\lambda_1 I} \quad \Theta_D = c_3 I e^{+\lambda_3 I} \\ v_S &= c_2 I e^{-\lambda_2 I} \quad \Theta_S = c_4 I e^{-\lambda_4 I} \\ k_D &= c_5 I e^{+\lambda_5 I} \quad n_D = c_7 I e^{+\lambda_7 I} \\ k_S &= c_6 I e^{-\lambda_6 I} \quad n_S = c_8 I e^{-\lambda_8 I} \end{aligned} \tag{2}$$

We can rationalize each of these formulas within the same picture. As injury, I, increases, damage will form faster, increasing v_D. The quantity of damage products will increase, and additional qualitative forms of damage will come 'on-line.' These changes will increase the threshold of damage (Θ_D), and affect the rate of damage clearance (k_D) and the coupling strength ('cooperativity') between different forms of damage (n_D). Since stress responses are activated by damage products, they will tend qualitatively and quantitatively to follow damage. However, stress responses are finite and will saturate, and will be subjected to increasing inhibition by damage. Therefore, v_S, Θ_S, k_S, and n_S initially increase with I but become less effective, and therefore decrease, as I further increases.

Substituting equation (2) into equation (1) gives the *general form* of our model:

$$\begin{aligned} \frac{dD}{dt} &= c_1 I e^{\lambda_1 I} \frac{(c_3 I e^{\lambda_3 I})^{c_7 I e^{\lambda_7 I}}}{(c_3 I e^{\lambda_3 I})^{c_7 I e^{\lambda_7 I}} + S^{c_7 I e^{\lambda_7 I}}} - (c_5 I e^{\lambda_5 I}) D \\ \frac{dS}{dt} &= c_2 I e^{-\lambda_2 I} \frac{(c_4 I e^{-\lambda_4 I})^{c_8 I e^{-\lambda_8 I}}}{(c_4 I e^{-\lambda_4 I})^{c_8 I e^{-\lambda_8 I}} + D^{c_8 I e^{-\lambda_8 I}}} - (c_6 I e^{-\lambda_6 I}) S \end{aligned} \tag{3}$$

Simplifying the General Model

While equation (3) captures all essential elements, it is too complicated. Guided by the intent to formulate a minimal model, we seek a simpler expression that preserves the qualitative dynamics. This can be accomplished by treating the v, k, and n parameters as constants. We set $v_D = v_S = k_D = k_S = 1$; we arbitrarily set $n_D = n_S = 4$, which generally can vary over a large range without affecting the qualitative dynamics. We leave only the Θ parameters as functions of I. Since they are inside of ratios, their absolute values cannot affect the scale of D and S, but the effect of I on the dynamics of D and S is preserved.

These simplifications have the effect that D and S will vary only between 0 and 1, so that the model output is *normalized*: at any value of I, the maximum values of D and S are 100% and the minimum values are 0%. In Supplementary Figure S2, we derive a version of the model that outputs absolute values of D and S. These are mathematically equivalent and interconvert via a scale factor. For the purpose of performing qualitative analysis, the normalized form is more suitable because the relevant dynamics is confined to the unit plane. Thus, for the remainder of the paper, we utilize the following simplified and normalized form where equation (3) is reduced to:

$$\begin{aligned}\frac{dD}{dt} &= \frac{(c_D I \mathrm{e}^{\lambda_D I})^4}{(c_D I \mathrm{e}^{\lambda_D I})^4 + S^4} - D \\ \frac{dS}{dt} &= \frac{(c_S I \mathrm{e}^{-\lambda_S I})^4}{(c_S I \mathrm{e}^{-\lambda_S I})^4 + D^4} - S\end{aligned} \tag{4}$$

Equation (4) constitutes our *minimal model* of cell injury dynamics. The symbols for the threshold parameters are renamed making them easier to associate with their meaning: $c_3 = c_D$; $\lambda_3 = \lambda_D$; $c_4 = c_S$; $\lambda_4 = \lambda_S$.

Understanding the Model

We here elaborate our interpretation of equation (4). The variables and parameters define the elements of our toy model. Solving equation (4) can be thought of as 'winding up' the toy model and letting it run, thereby exposing the dynamics of equation (4) to biological interpretation.

There are two elements represented by equation (4): (1) a cell (as described above, with a phenotype and an intracellular black box) and (2) a damage agent. Together, these form an *injury system* where a damage agent is applied to a cell, thereby injuring it. The cell is defined by the parameters c_S and λ_S, which characterize only the cell's intrinsic stress responses: larger c_S and smaller λ_S indicate a stronger cell. The lethality of the damage agent is defined by c_D and λ_D: if both are larger, the damage agent is more toxic. Thus, a specific injury system is defined by four numbers: two define the damage agent (c_D, λ_D), and two define the cell type (c_S, λ_S). The amount of damage agent applied to the cell is given by I. The cell's response to injury is given by the variables D and S.

On running the toy model, an injury is enacted in three stages: (1) the damage agent injures the cell, thereby (2) setting the D–S competition in motion inside the cell, where either D or S wins, followed by (3) the biological consequence that the cell either recovers or dies. We discuss each stage in turn.

Application of the damage agent to the cell—injuring the cell—informally can be thought of as applying a 'kick' of strength I to the cell, inducing the D–S competition. Formally, in equation (2), I is not a function of time, constituting one of our minimal modeling assumptions. Therefore, equations (3) and (4) are autonomous ODEs treating injury I as an externally imposed perturbation applied to the cell at time zero, resetting D and S to change via equation (4).

The initial condition of an uninjured cell is the homeostatic phenotype $(D, S) = (0, 0)$; that is, there is no damage or activated stress responses. Injury disturbs homeostasis, making the cell unstable (Lipton, 1999). Equation (4) outputs two simultaneous time courses, one for D and one for S. The point (D, S) at each time t gives the *trajectory* of the D–S competition, describing the cell's deviation from homeostasis as a path, successive points of which represent successive states of the cell's instability.

End points of trajectories are called *fixed points* because the rate of change of the system is zero (Supplementary Figure S3). In our model, the end point of a D–S trajectory, designated (D^*, S^*), is the maximum deviation of the cell from homeostasis, its state of maximum instability. The duration from the initial state $(0, 0)$ to the state of maximum instability (D^*, S^*) is the duration of the D–S competition, which we call the *competition time*, t_C.

Without additional modeling assumptions, the system would stay frozen at (D^*, S^*) forever. But this does not happen in real injury systems. Since, at (D^*, S^*) the cell cannot deviate any further from homeostasis, we interpret (D^*, S^*) to be the point where the effect of I on D and S ceases: the 'force' of the 'kick' is exhausted at (D^*, S^*). We therefore assume that precisely at (D^*, S^*), the value of I becomes zero.

Then, because the effect of I ceases, and because the state (D^*, S^*) is inherently unstable for the cell, D and S do not remain stationary. Instead, the system seeks to regain stability by 'falling back' to $(0, 0)$. The descent to $(0, 0)$, we give two mutually exclusive interpretations. If $S^* > D^*$ then $(0, 0)$ represents recovery to the cell's initial homeostatic steady state. If $D^* > S^*$, $(0, 0)$ represents death, an oblique form of stability because the cell no longer exists. We thus use the fixed point (D^*, S^*) to map a gradation of injury magnitudes to the binary outcome of recovery or death.

It takes time to decay from (D^*, S^*) to $(0, 0)$. This is the *time of recovery* (t_R) if $S^* > D^*$, or the *time to death* (t_D) when $D^* > S^*$. The rate the cell decays

from (D^*, S^*) to $(0,0)$ can be inferred as follows. If $S^* >> D^*$ (their difference is relatively large) then the minimal damage will be cleared and repaired quickly, and recovery is rapid. If $D^* >> S^*$, the damage will so overwhelm the cell that it will die quickly. When S^* and D^* are closer in magnitude, it will take longer for each to overcome the other. Thus, the recovery/death rates are inversely proportional to the magnitude of the difference between D^* and S^*. We can calculate t_R and t_D by:

$$t_R = \frac{\ln(S^*/S_f)}{|D^* - S^*|} \text{ when } S^* > D^*$$
$$t_D = \frac{\ln(D^*/D_f)}{|D^* - S^*|} \text{ when } D^* > S^* \quad (5)$$

Where $D_f = S_f \sim 0$ are the final values of D and S. In practice, we set $D_f = S_f = 10^{-6}$ and consider D and S to be 0 when they are 1 part per million of their maximum value, which, in the normalized equation (4) cannot exceed 1.

Thus, equation (4) is first solved to obtain the time courses of the D–S competition and the value (D^*, S^*). (D^*, S^*) is then used in equation (5) to calculate t_R or t_D. This procedure is illustrated in Figure 3. I drives the D–S competition as a step function, equal to a nonzero value I_0 up to t_C. After t_C, the effect of I is spent ($I = 0$) and the system passively reverts to $(0,0)$ via equation (5). The resultant time courses are concatenated to give the full injury time course. Figures 3B–3D illustrate plots of D and S time courses across a range of I values; in Part 2 multiple time course are displayed as in Figure 3D.

Part 2: Qualitative analysis of the cell injury model

Discussing equation (4) output is a necessary step toward understanding the therapeutic implications of the model. In modern dynamics, *qualitative*

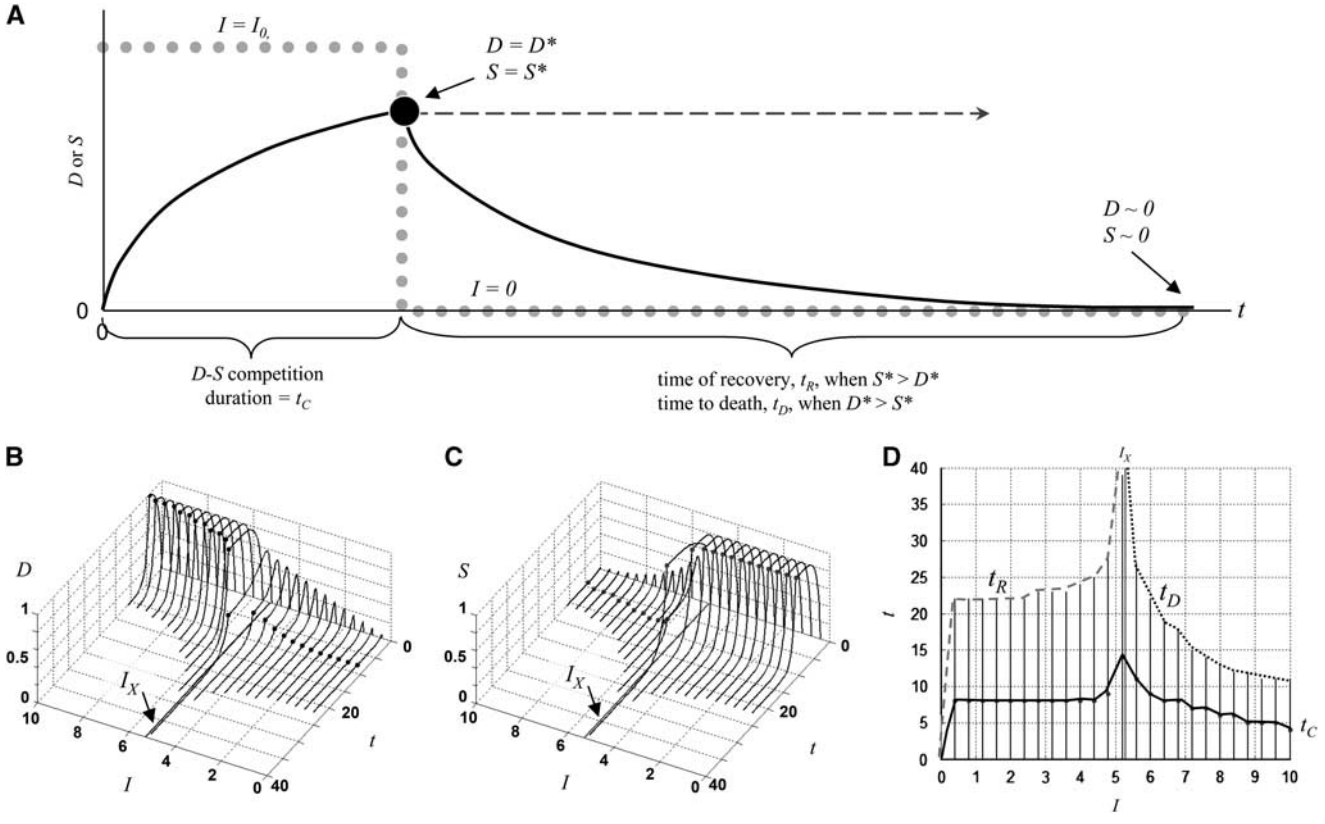

Figure 3 (**A**) The total time course of cell injury consists of two concatenated steps. Shown is a typical time course for either D or S. Gray dotted line shows I as a step function. During the D–S competition, I is a nonzero value I_0. The duration of the D–S competition is the *competition time*, t_C. At t_C, equation (4) reaches the fixed point solution (D^*, S^*). After t_C, I is set to zero and the system passively decays from (D^*, S^*) to $(0,0)$ as described by equation (5), where the decay rate is $|D^* - S^*|$. When $S^* > D^*$, the duration to $(0,0)$ is the *recovery time*, t_R. When $D^* > S^*$, the duration is the *time to death*, t_D. Dashed line shows how (D^*, S^*) would continue as a straight line to $t = \infty$ if I was not treated as a step function. (**B**) Example of a series of D time courses over an injury course. The black point on each time course is D^* and occurs at $t = t_C$, showing how t_C varies with I. (**C**) The corresponding series of S time courses over the same injury course. The black point on each time course is S^* and occurs at $t = t_C$ for each I. (**D**) Plots of time, t, versus injury, I. The line labeled t_C corresponds to the black points in (**B**, **C**). After t_C, all durations left of I_X are t_R, and to the right of I_X are t_D. For (**B**–**D**), the parameters used in equation (4) are $c_D = 0.1$, $\lambda_D = 0.1$, $c_S = 20$, $\lambda_S = 0.9$, $0 < I < 10$. $I_X = 5.3$.

analysis is the study of bifurcation diagrams: wherein the shift in position and the quality (stable or unstable) of the fixed points are plotted as a function of a parameter of interest (Strogatz, 1994). For nonmathematicians, tutorials on nonlinear ODEs, qualitative analysis, etc. are provided in Supplementary Figures S3–S5.

We are interested in understanding how specific injury systems behave as I increases, and thus solve equation (4) holding $(c_D, \lambda_D, c_S, \lambda_S)$ at fixed values, while varying I. We call this an *injury course*: the response of a specific injury system from low to high I values. Mathematically, an injury course is simply a bifurcation diagram of equation (4) where I is the control parameter used to construct the bifurcation diagrams.

Injury Courses Come in Four Varieties

Equation (1) is well known to display bistable dynamics (Huang *et al*, 2007; Chatterjee *et al*, 2008), that is, solutions with two fixed point attractors and their corresponding repeller. Equation (4) retains this feature. Depending on the values of the parameters $(c_D, \lambda_D, c_S, \lambda_S)$, equation (4) outputs one of four qualitatively different injury courses: one is monostable and three contain different patterns of bistability. We now present examples of each, displayed as D^* versus I and S^* versus I bifurcation diagrams, and as (t_R, t_D) versus I plots, where time courses are calculated from initial conditions $(D_0, S_0) = (0, 0)$.

1. Monostable Injury Courses: Here, a single attractor (D^*, S^*) exists at each value of I in the injury course. We consider how the attractor (D^*, S^*) changes with I. In Figure 4A, for the values of injury $I < \sim 2.5$, $D^* = 0$ and $S^* = 1$, indicating that at the end of the D–S competition, the stress responses are at their peak value (normalized to 100%) and total damage is 0. For all $I > \sim 10$, the opposite occurs: $D^* = 1$ and $S^* = 0$, so damage is maximal and the stress responses are completely suppressed. In the intervening range of $\sim 2.5 < I < \sim 10$, D^* increases continuously from 0 to 1, and S^* decreases continuously from 1 to 0. The bifurcation diagrams trace out sigmoidal curves, demonstrating the nonlinearity of the dynamics.

The most significant feature of the injury course is that there exists one specific value of I at which $D^* = S^*$, occurring in this example at $I = 6.9$. For all $I < 6.9$, $S^* > D^*$ and the system will recover. For all $I > 6.9$, $D^* > S^*$, and the system is fated to die. Thus, the magnitude of I where $D^* = S^*$ is the tipping point between life and death of the injured system. We call this the *crossover value of I* and designate it I_X.

I_X, that value of I where $D^* = S^*$, is a characteristic feature of all four varieties of injury course. One advantage of the normalized equation (4) is that a simple and exact formula to calculate I_X is available:

$$I_X = \frac{\ln c_S - \ln c_D}{\lambda_D + \lambda_S} \qquad (6)$$

Significance of Being Able to Calculate I_X

Equation (6) is significant for many reasons. First, it satisfies our intuition that, for any type of injury, there will be some exact magnitude of injury, I_X, which is the tipping point between life and death. This idea is usually expressed intuitively as the 'cell death threshold.' Our model shows that it is a precise and calculable value on an injury course and gives the exact method to calculate it: I_X is the value of I where $D^* = S^*$.

Theoretically, equation (6) makes clear that the tipping point between life and death is a combined function of the cell type (c_S, λ_S) and the damage agent (c_D, λ_D). Different combinations of cell types and damage agents, represented by different values for (c_S, λ_S) and (c_D, λ_D), respectively, will produce different values of I_X. This has empirical implications for comparing the same insult across species. If (c_S, λ_S) are different between homologous cell types of two species (say CA1 neurons in human and rat), then I_X will be different, even if the insult is the same. Then, pharmacological treatments effective in one species would not translate to another, unless scaled to account for different values of I_X.

Being able to calculate I_X also has clinical implications. If a particular clinical condition occurs with respect to some cell type at $I < I_X$, the cell will deterministically recover and medical intervention is not, in principle, required. If the system manifests $I > I_X$, the system will deterministically die. Thus, knowing precisely the range $I > I_X$ provides a 'hard target' at which to aim therapeutic efforts.

Time Courses of Monostable Injury Courses

When we consider the corresponding D and S time courses across the I range, t_R and t_D are approximately mirrored through the line $I = I_X$ (Figure 4A, 3rd panel). Monostable injury courses show recovery durations, t_R, asymptotically approaching infinity at I_X. The time to death, t_D, asymptotically descends from infinity at $I > I_X$. Stated simply, in a monostable injury course, the recovery times and times to death are of relatively long durations around I_X.

Of therapeutic significance, D and S follow different time courses for each I, indicating that different lethal injury magnitudes are not identical, and implying they cannot be treated identically. For example, a treatment that is effective at inhibiting cell death at 10 minutes may be ineffective at 12 minutes of global ischemia. Part 3 is dedicated to elaborating this important insight.

We note that, for monostable injury courses, I_X calculated via equations (4) and (5) is a physically unrealizable state. An injured system perfectly balanced between total damage, D, and total stress responses, S (i.e., $D^* = S^*$) would take an infinite amount of time to resolve, and nonsensically, would resolve to neither recovery nor death.

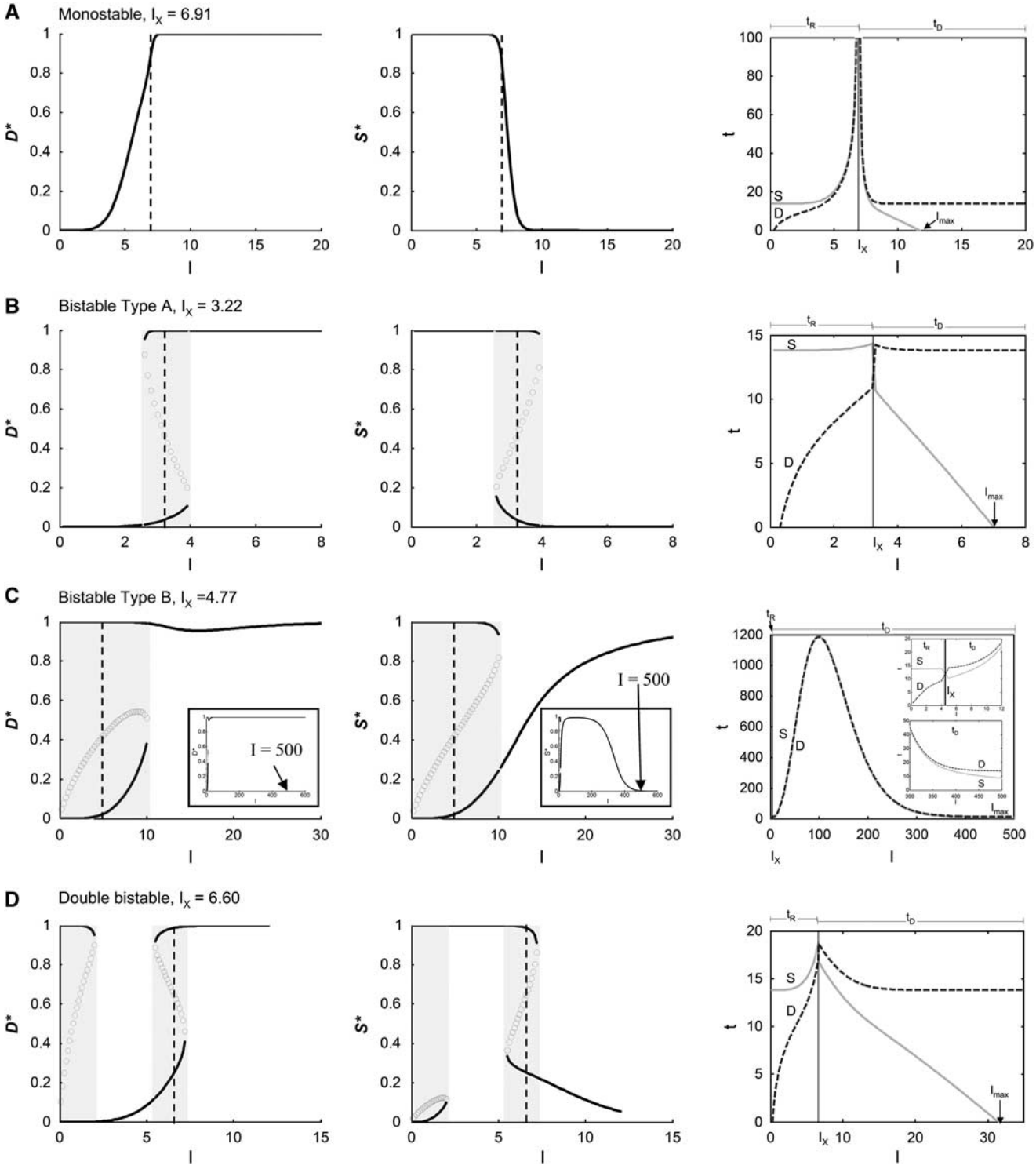

Figure 4 Illustration of the four types of *injury courses* to emerge from equations (4) and (5). Rows (**A**–**D**) are monostable, type A bistable, type B bistable, and double bistable injury courses, respectively. First and second panels of each row are bifurcation diagrams of D^* versus I and S^* versus I, respectively. Dashed vertical lines indicate the value of I_X, and gray areas indicate regions of bistability, with repeller points indicated with open circles. Arrows in panel **A** indicate I_{max}, the value of I where $(D^*, S^*) = (1, 0)$ and can be considered the functional end point of the injury course since for all $I > I_{max}$, $(D^*, S^*) = (1, 0)$. Insets in panels 1 and 2 of (**C**) show the full I range of the type B bistable injury course and indicate $I_{max} \sim 500$. Third panel in each row are t_R, t_D versus I plots. I_X is indicated by solid vertical lines. Top inset in panel 3 of (**C**) shows blow-up around I_X, and bottom inset shows blow-up around I_{max}. The values c_D, c_S, λ_D, and λ_S, used to generate (**A**–**D**), are $[0.1, 100, 0.1, 0.9]$, $[0.1, 2.5, 0.1, 0.9]$, $[0.075, 0.0825, 0.01, 0.01]$, and $[0.1, 0.4, 0.02, 0.19]$, respectively. The parameter I varied as indicated on each axis.

2. Bistable Injury Courses, Type A: In this dynamical pattern, the system bifurcates from monostable to bistable phase planes (Supplementary Figures S4 and S5) over a subrange of the injury course. The bistable region (Figure 4B, gray areas) resembles an S-shape in D^* versus I plots, and a mirrored S-shape in S^* versus I plots, consisting of lower and upper arms of attractor points connected by the repeller points. Unlike monostable injury courses where the transition to death is continuous as the system approaches I_X, with this injury course, the transition to cell death at I_X is abrupt and discontinuous.

The bistable type A time courses (Figure 4B) do not show increasing durations around I_X due to the bistability. At $I = I_X$, the relationship $D^* = S^*$ manifests as the repeller and not the attractor points, and only attractor points are used in equation (5). Thus, I_X is again a physically unrealizable state. The net result in this example is that t_R and t_D remain roughly constant across the entire injury course, a very different dynamics from the monostable injury course.

3. Bistable Injury Courses, Type B: Here, the bistability begins at $I = 0$ and extends into the I range (Figure 4C). Bistability starting at the origin means that there is potential for the system to die at all injury magnitudes (elaborated in Part 3). Additionally, this injury course has the unique characteristic that S^* increases *after* I_X. For a large range of $I > I_X$, the system, even though fully determined to die, will persist for significant durations.

For the bistable type B dynamical pattern, the D and S time courses appear similar, showing a large 'hump' after I_X, when plotted at full scale of the injury course (Figure 4C, 3rd panel). However, the time courses are not identical and for $I > I_X$, $D^* > S^*$ and the system will die (Figure 4C, insets).

4. Double Bistable Injury Courses: Here, two regions of bistability occur in the injury course (Figure 4D). The type B bistable region extends from the origin, and a type A occurs after a monostable range of I. I_X occurs in the type A bistable region, so the dynamics of this system is discontinuous at I_X. The D and S time courses thus resemble those of type A with t_R and t_D roughly constant across the injury course. Again, because of bistability at the origin, this injury system can potentially die at injury magnitudes $I < I_X$.

The Four Injury Course Dynamics Are Not Independent

The intimate relationship of the four injury course dynamics is illustrated in Supplementary Figure S6, which shows bifurcation analysis varying one additional system parameter (c_S) along with I. The four dynamical patterns described above are related as cross-sections of 2D surfaces in parameter space, and gradually transform into one another. Thus, the model outputs many variations of the four basic injury course patterns and reveals a family concept of injury dynamics that is perhaps unnoticeable from an idiosyncratic biological viewpoint.

Delayed Death After Injury

An immediate application of the above concepts is that they provide a dynamical explanation, independent of biological details, for the delayed neuronal death phenotype characteristic of ischemic brain injury (Kirino, 2000). The delay duration simply indicates a lethal value of I where D^* is only slightly greater than S^* (e.g., $|D^* - S^*|$ is a relatively small number), thus taking a longer time to resolve to death. The model shifts focus from the observation that some value of I produces a long time to death, t_D, to the question: on what type of injury course does that I value lay?

Part 3: Therapeutic implications of the dynamical model of cell injury

In general, therapeutics seeks to slow, or preferably, reverse the progression to death of an injured system. Most therapeutic strategies attempted on multifactorial injury systems derive from empirical studies conducted at one, or a few injury magnitudes, and are formulated in terms of the qualitative biological details of a given tissue pathology (e.g., free-radical scavenger, apoptosis inhibitor, etc.). But the system is multifactorial: as details accumulate, cause and effect become opaque. Instead of details, we link the universal properties of injury magnitude to outcome via D and S, and obtain transparent access to the injury course dynamics. Therapeutics becomes manipulation of injury dynamics, and biological details take their place as the levers of these manipulations.

We now discuss the therapeutic application of the model. First, we model preconditioning and illustrate in concrete terms how therapeutics shifts a pro-death to a pro-survival trajectory by altering the initial conditions in bistable phase planes. We gain the insight that common empirical manipulations, like preconditioning or pharmacologic treatments, can be interpreted as solving equation (4) under different initial conditions. Knowing this we then ask: given a bistable injury course, what initial conditions are required to ensure survival at lethal injury values $I > I_X$? We show that as I increases over I_X, progressively larger shifts in initial conditions are required to generate a survival outcome. This result provides a plausible explanation why so many therapeutic manipulations work in the laboratory but fail in the clinic.

Preconditioning and Initial Conditions

Preconditioning is a general response of cells to a wide variety of damage agents (McDunn and Cobb,

2005), referring to a state where a system exposed to a sublethal injury can, within a fixed time window, survive a second, lethal injury. Different damage agents can substitute for each other. Such 'cross-induction,' and the ubiquity of this phenomenon, suggests that a universal dynamic operates independent of biological specifics. We now mathematically simulate preconditioning by showing a system survive a lethal injury $I > I_X$ after exposure to a sublethal injury $I < I_X$.

Figure 5 illustrates an injury system where the tipping point $I_X = 3.22$. Figures 5A and 5B show pairs of D and S time courses, at lethal $I = 3.5$ ($> I_X$) and sublethal $I = 2.5$ ($< I_X$), respectively. In Figure 5A, D dominates, and the time to death occurs at $t_D \sim 25$. In Figure 5B, S dominates, and the system fully recovers at $t_R \sim 20$. In the sublethal case, there is a range of times, t_P (times which gives rise to preconditioning), marked by the gray box, where $D \sim 0$ and $S > 0.25$. If the system is subjected to a second, lethal injury $I = 3.5$ at any time over this period, it will survive.

Specifically, if the system in Figure 5B is subject to a second, lethal insult $I = 3.5$, exactly at the time designated by (*) (which is within the t_P window), the resulting D and S time courses exhibit the behavior shown in Figure 5C. S now dominates, $t_R \sim 30$, and the system exposed to the lethal insult now survives. This preconditioning-like result is achieved by taking the values $D = 0$ and $S = 0.25$ from the sublethal case precisely at the time the lethal insult is induced (at *), using these as the *initial conditions* for solving equation (4), and generating the time courses in Figure 5C. While both Figures 5A and 5C are injured at the lethal $I = 3.5$, Figure 5A uses initial conditions $(0, 0)$, but Figure 5C uses initial conditions $(0, 0.25)$. By simply changing initial conditions, the system is made to 'flip state' from death to recovery.

The effect of initial conditions is evident by visual inspection of the phase plane at $I = 3.5$ (Figure 5D). Trajectories started from $D_0 = 0$ and $S_0 > 0.25$ (gray curves) end at the survival attractor, but trajectories started from $D_0 = 0$ and $S_0 < 0.25$ (black dashed curves) end at the death attractor.

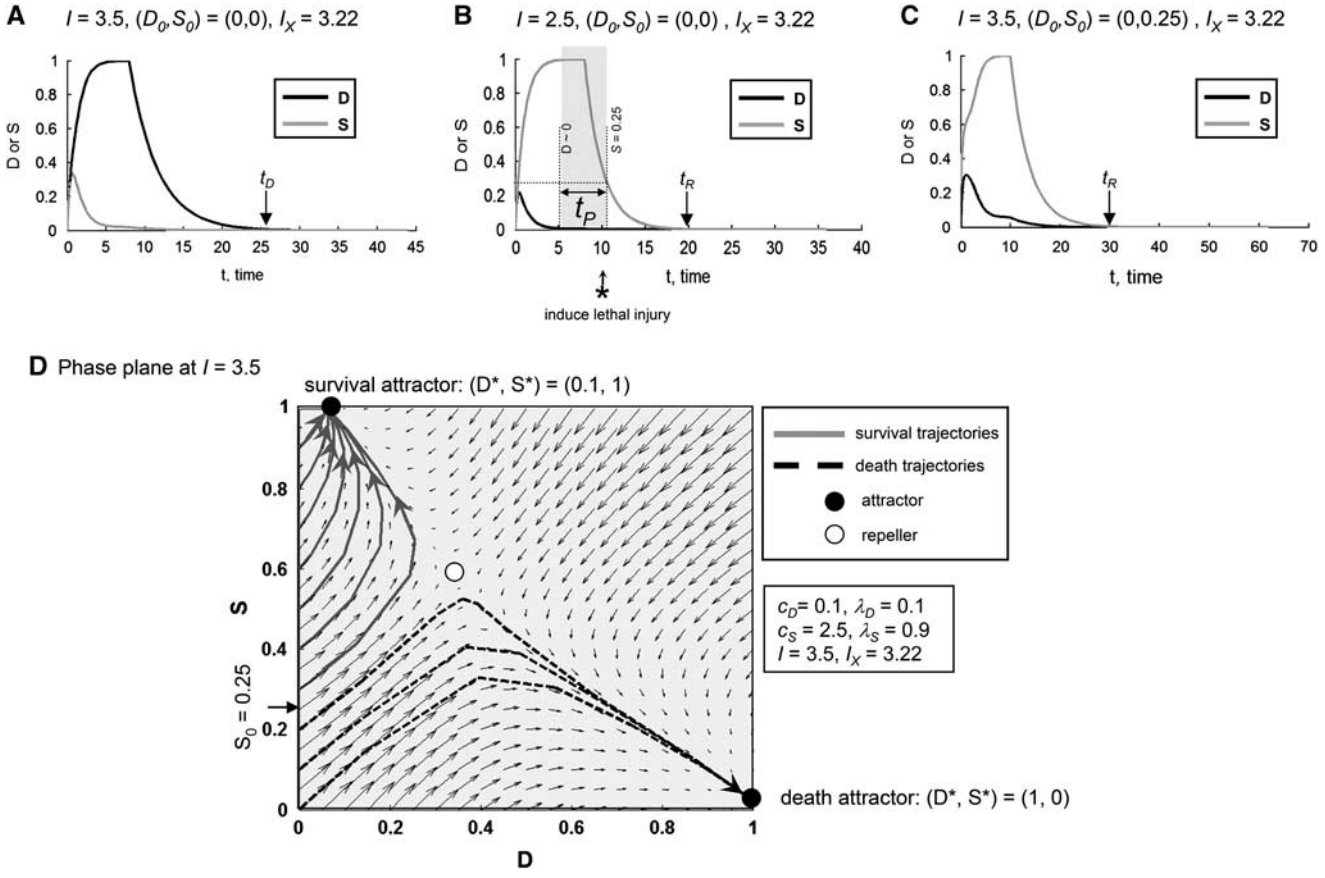

Figure 5 Simulating a preconditioning-like effect with equation (4) and (5). (**A**) D and S time courses at a lethal value of $I = 3.5$ using initial conditions $(0, 0)$. (**B**) D and S time courses at a sublethal value of $I = 2.5$ using initial conditions $(0, 0)$. Gray box marks t_R the range of durations for which the system will survive a second, lethal injury of $I = 3.5$. (*) Indicates time of inducing a 2nd, lethal injury of $I = 3.5$. (**C**) D and S time courses for $I = 3.5$ using initial conditions $(0, 0.25)$. For (**A**–**C**), t_R and t_C are marked when $D = S \sim 0$. (**D**) Phase plane for $I = 3.5$. Attractors: black circles; repeller: white circle at indicated coordinates. Gray curves: trajectories to the survival attractor; black dashed curves: trajectories to the death attractor. Parameters used to generate phase plane and time courses in (**A**–**C**) are indicated, and are the same parameters used to generate the type A bistable injury course in Figure 4B.

Thus, the role of sublethal injury in preconditioning is simply to put the cell in a state where $S>0$ for some duration while $D\sim 0$, this state serving as altered initial conditions under which the second (normally) lethal insult is induced. Survival results solely from the altered initial conditions generating a pro-survival trajectory on the bistable phase plane. Notably, the fundamental thresholds of the system,

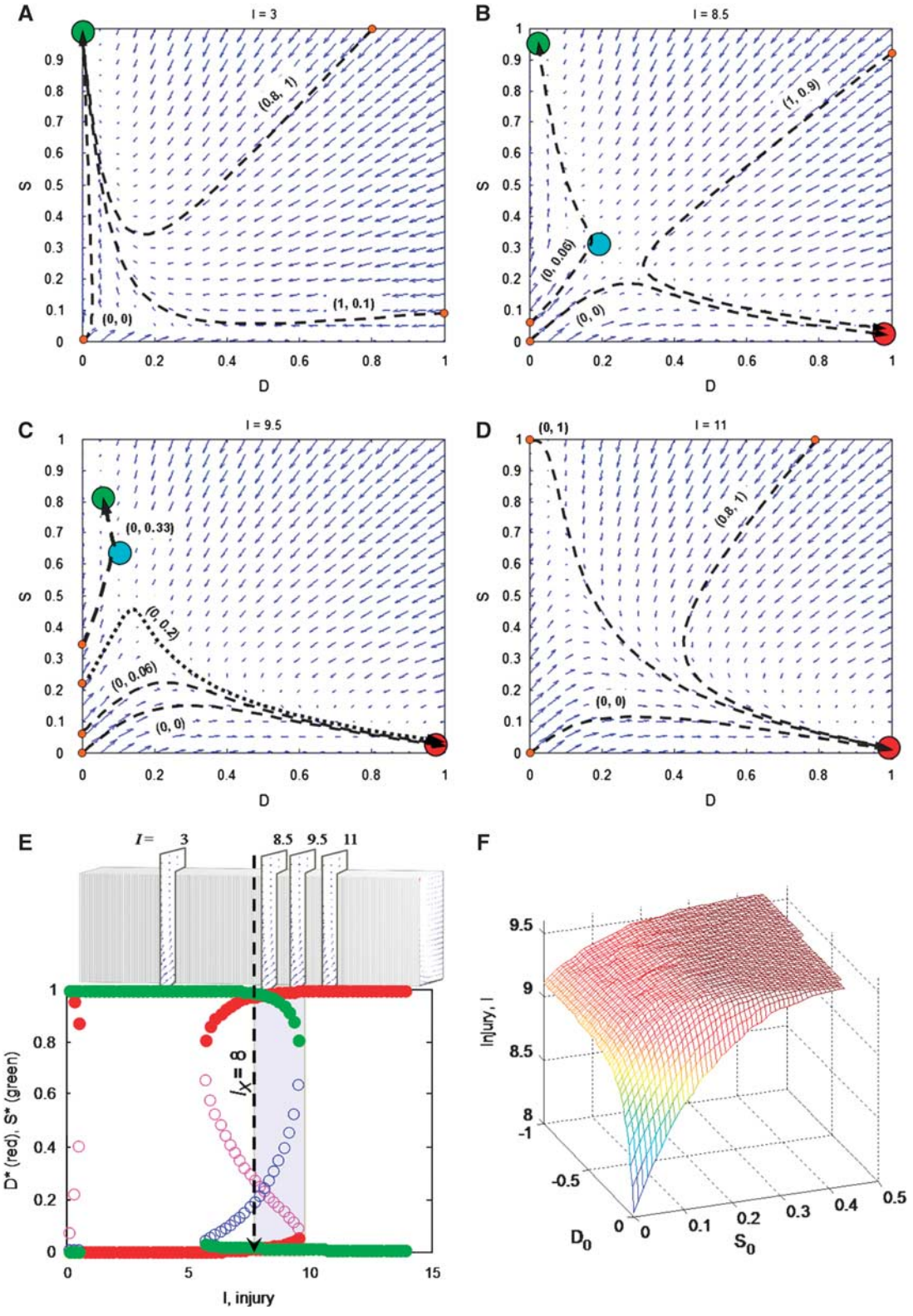

Θ_D, Θ_S, and the tipping point I_X (e.g., 'cell death threshold') remain unchanged. As well they should: these thresholds are intrinsic properties of the *injury system* (see equation (6)) and not of any specific injury magnitude.

Initial Conditions and Therapeutic Manipulations

It is obvious from the preconditioning example that survival cannot be achieved in a lethal monostable phase plane: there is no survival attractor to which the system can be diverted. Thus, flipping state from a death to a survival outcome requires a bistable phase plane. Our minimal model thus succeeds in capturing what is arguably the most important aspect of injury dynamics: It offers the general explanation that therapy, the conversion of a normally lethal injury into a nonlethal one, is the conversion of a pro-death trajectory to a pro-survival trajectory by altering initial conditions on a bistable phase plane.

In Supplementary Figure S7, we illustrate the opposite effect: a system can be made to die at (normally) sublethal $I<I_X$ in a bistable phase plane when $D_0>0$. $D_0>0$ indicates preexisting damage, thus simulating comorbidity (as alluded above for type B and double bistable injury courses). A physical example might be the worsened stroke outcome of diabetics compared with nondiabetics.

Thus, an injury system in a bistable phase plane can be made to 'flip state' by altering the initial conditions to equation (4). Different initial conditions can be mapped to common empirical manipulations used to study cell injury, that either inhibit or enhance cell death:

1. $D_0>0$ would simulate comorbidity, or preexisting damage before application of injury, I. This will enhance cell death.
2. $D_0<0$ simulates a pretreatment with a drug that inhibits damage, therefore inhibiting cell death.
3. $S_0>0$ models preconditioning, inhibiting cell death, as discussed above, but can also include genetic overexpression of protective proteins (e.g., HSP70).
4. $S_0<0$ can simulate gene knockouts or mutations of stress response proteins, which enhance the proclivity to cell death.

In each of these cases, there is some manipulation performed before the application of the lethal injury, I, and thus represent 'pretreatments.' A discussion of how to manipulate a trajectory once it is initiated (i.e., a 'post-treatment') is beyond our present scope.

1,026 Reevaluated

In practice, injury systems are standardized to a single lethal injury magnitude, which then is analyzed in great detail. For example, 10 minutes is the standard lethal injury for CA1 neuron death in the study of rat global brain ischemia. This approach, however, reveals nothing about injury course dynamics. The preconditioning example demonstrates that salvage is only possible in a bistable phase plane. The injury course then becomes all-important for a general therapeutic approach because it reveals precisely the range of injury magnitudes, if any, that possess bistable dynamics.

Let us consider further, within the context of the model, the implications of standardizing on a single lethal injury magnitude. When lethal injury is induced on an uninjured animal with no pretreatments, this will produce a single pair of D and S time courses, started from initial conditions $(0,0)$. However, a single trajectory from $(0,0)$ at a single lethal I does not provide enough information to determine if the phase plane is bistable or monostable. To make this determination, one can manipulate initial conditions at that lethal I, as described above. If the outcome can be changed from death to survival, this is *de facto* evidence that the system dynamics is bistable. Inability to flip state indicates a monostable phase plane. But whether we determine that a single lethal value of I is bistable or monostable, we are still dealing with only a single-phase plane. What happens when we consider other lethal values of I (e.g., all $I>I_X$)? Does the protection obtained at the standard experimental lethal value of I carry over to other lethal values?

We therefore consider a bistable injury course that is mathematically defined beforehand. Figure 6 shows a doubly bistable injury course where $I_X=8.0$ and the lethal bistable region extends from $8.0<I<9.6$. The bifurcation diagram in Figure 6E derives from a

Figure 6 Larger shifts in initial conditions are required to flip an injury system from a pro-death to a pro-survival trajectory as I increases past I_X. Phase plane solutions to equation (4) at (**A**) $I=3$, a monostable survival phase plane; (**B**) $I=8.5$, a lethal bistable phase plane; (**C**) $I=9.5$, a lethal bistable phase plane; and (**D**) $I=11$, a lethal monostable phase plane. For (**A**–**D**), vector fields are shown as blue arrows. Survival attractors are green circles, death attractors are red circles, and repellers are blue circles. Each phase plane shows trajectories (dashed lines) from initial conditions as indicated, and the locations of the initial condition points are shown by small orange circles. (**E**) Bifurcation diagram for entire injury course, with D^* and S^* versus I plots on the same graph. D^* attractors: red; D^* repellers: magenta open circles; S^* attractors: green; S^* repellers: blue open circles. $I_X=8.0$ as indicated with dashed vertical line. Purple area in bifurcation diagram is *therapeutic range* where the system is lethal from initial conditions $(0,0)$, but is bistable and therefore contains both a pro-survival and pro-death attractor. Above the bifurcation diagram, the phase planes are depicted as a stack for which the four-phase planes in (**A**–**D**) are extruded and labeled accordingly, showing the position of the respective phase planes on the injury course. (**F**) Plot of initial conditions $S_0>0$ and $D_0<0$ that will cause a pro-survival outcome in the therapeutic range from $I=I_X$ to the end of the bistable range at $I\sim9.6$. Coloring indicates height, with blue end of rainbow corresponding to I values close to I_X and red end for I close to the end of bistable region at $I=9.6$.

Table 1 Initial conditions required to effect survival for lethal *I*, for the injury course given in Figure 6 in which $I_X = 8$

I	D_o	S_o	*% Preactivated stress responses*
8.04	0	0.00001	10^{-3}
8.1	0	0.01	1
9.0	0	0.14	14
9.5	0	0.33	33
>9.6	0	—	—

continuum of phase planes across the continuum of injury magnitudes. Figures 6A–6D illustrate individual phase planes at values of I whose positions are indicated in the bifurcation diagram in Figure 6E. In the sublethal monostable phase plane $I = 3$ (Figure 6A), all trajectories end at the single survival attractor; there is nowhere else to go. Similarly, in the lethal monostable phase plane $I = 11$ (Figure 6D), all trajectories end at the single death attractor.

Figures 6B and 6C show bistable phase planes that are lethal from initial conditions $(0, 0)$. At $I = 8.5$, changing initial conditions from $(0, 0)$ to $(0, 0.06)$, flips outcome to survival. However, at $I = 9.5$, the initial conditions $(0, 0.06)$ do not effect survival. At $I = 9.5$, initial conditions must be $(0, 0.33)$ to flip state. For all $I > 9.6$, no change in initial conditions can effect survival because there are no survival attractors. The bistable region marked by the purple rectangle in Figure 6E is the *therapeutic region* of the injury course: those lethal values of I susceptible to successful therapy.

One can also obtain survival by setting $S_0 = 0$ and taking D_0 negative (e.g., inhibiting damage). Figure 6F plots all combinations of $S_0 > 0$ and $D_0 < 0$ that will effect survival over the therapeutic region of the injury course. This plot approaches $(0, 0)$ at I_X and fans out as I increases past I_X, showing in full what the phase planes in Figures 6B and 6C illustrated in a more limited way: As I increases past I_X, the initial conditions must progressively increase in magnitude to cause a survival outcome. In short, each value of I in the therapeutic region requires different initial conditions to effect survival.

Table 1 lists specific values from Figure 6F. At an infinitesimal past I_X, $I = 8.04$, S_0 need only be trivially small—stress responses need be activated to only 1/1,000th of a percent—to cause the system to survive. The preactivation of stress responses must increase dramatically with I to generate a survival trajectory: at $I = 9.5$, stress responses must be preactivated to 33%. This is 33,000 times greater than at $I = 8.04$.

These results offer a plausible explanation why 'anything' acts as a neuroprotectant in laboratory animal models of brain ischemia, but none of these treatments has been successful when taken to clinical trials. If the experimental models use lethal values of I close to I_X, then a trivially small change in initial conditions, by either increasing S_0 or decreasing D_0 will convert a lethal trajectory to a survival trajectory. However, in clinical trials, the patient population displays heterogeneity of injury magnitudes, I. If we assume for argument's sake that all lethal magnitudes $I > I_X$ (at least those consistent with remaining alive) are represented with an equal frequency in the clinical subject population, then only subjects with lethal injury $I \sim I_X$ will respond to the treatment. All others will be unresponsive if the therapy was developed in experimental models where the injury was close to I_X. Averaging this heterogeneous population of injury magnitudes with respect to outcome will clearly result in no effect.

Thus, without a preexisting knowledge of the injury course, without knowledge of the range of injury magnitudes that are bistable, without knowledge of the precise initial conditions to effect a survival outcome at each I in the therapeutic range, and without knowledge of how I_X scales between the experimental animal models and humans, any clinical trial design not taking these factors into account has a vanishingly small probability of success.

Summary and conclusions

We presented a minimal ODE system that embodies a general theory of cell injury dynamics. It provides a quantitative and systematic framework to determine the dynamics of specific cell injury systems. This model introduces the language and concepts of nonlinear dynamics to the study of cell injury, the benefit of which have been conveyed by the examples. The important next step is to operationalize the model for application in the laboratory, with an eye on the clinical arena. The implication is the development of a new breed of clinical trial operating at a more sophisticated theoretical level by using formal predictive models. With such an approach, and with some luck, we may be able to emulate the success of our scientific colleagues in the physical sciences.

Acknowledgements

The authors thank Gerald Dienel for helpful comments on a draft of this work; the two anonymous reviewers for helping us clarify important issues; Peter Lipton for first suggesting applying dynamics to brain ischemia; and Thaddeus Wieloch for his seminal insights.

Disclosure/conflict of interest

The authors declare no conflict of interest.

References

Alon U (2006) *An Introduction to Systems Biology: Design Principles of Biological Circuits*. London, UK: Chapman & Hall/Crc

Chatterjee A, Kaznessis YN, Hu WS (2008) Tweaking biological switches through a better understanding of bistability behavior. *Curr Opin Biotechnol* 19:475–81
DeGracia DJ (2010*a*) Towards a dynamical network view of brain ischemia and reperfusion. Part I: background and preliminaries. *J Exp Stroke Transl Med* 3:59–71
DeGracia DJ (2010*b*) Towards a dynamical network view of brain ischemia and reperfusion. Part II: a post-ischemic neuronal state space. *J Exp Stroke Transl Med* 3:72–89
DeGracia DJ (2010*c*) Towards a dynamical network view of brain ischemia and reperfusion. Part III: therapeutic implications. *J Exp Stroke Transl Med* 3:90–103
DeGracia DJ (2010*d*) Towards a dynamical network view of brain ischemia and reperfusion. Part IV: additional considerations. *J Exp Stroke Transl Med* 3:104–14
Dirnagl U, Meisel A (2008) Endogenous neuroprotection: mitochondria as gateways to cerebral preconditioning? *Neuropharmacology* 55:334–44
Hossmann KA (2009) Pathophysiological basis of translational stroke research. *Folia Neuropathol* 47:213–27
Huang S (2009) Reprogramming cell fates: reconciling rarity with robustness. *BioEssays* 31:546–60
Huang S (2011) Systems biology of stem cells: three useful perspectives to help overcome the paradigm of linear pathways. *Philos Trans R Soc Lond B Biol Sci* 366:2247–59
Huang S, Guo YP, May G, Enver T (2007) Bifurcation dynamics in lineage-commitment in bipotent progenitor cells. *Dev Biol* 305:695–713
Huang S, Wikswo J (2006) Dimensions of systems biology. *Rev Physiol Biochem Pharmacol* 157:81–104
Kaplan D, Glass L (1995) *Understanding Nonlinear Dynamics*. New York, NY: Springer
Kirino T (2000) Delayed neuronal death. *Neuropathology* 20(Suppl):S95–7
Lipton P (1999) Ischemic cell death in brain neurons. *Physiol Rev* 79:1431–568
McDunn JE, Cobb JP (2005) That which does not kill you makes you stronger: a molecular mechanism for preconditioning. *Sci STKE* 291:pe34
O'Collins VE, Macleod MR, Donnan GA, Horky LL, van der Worp BH, Howells DW (2006) 1,026 experimental treatments in acute stroke. *Ann Neurol* 59: 467–77
Philip M, Benatar M, Fisher M, Savitz SI (2009) Methodological quality of animal studies of neuroprotective agents currently in phase II/III acute ischemic stroke trials. *Stroke* 40:577–81
Picht P (1969) *Mut zur Utopie*. Munich: Piper
Savitz SI (2007) A critical appraisal of the NXY-059 neuroprotection studies for acute stroke: a need for more rigorous testing of neuroprotective agents in animal models of stroke. *Exp Neurol* 205:20–5
Strogatz S (1994) *Nonlinear Dynamics and Chaos*. Reading, Massachusetts: Perseus Books
Tyson JJ, Chen K, Novak B (2001) Network dynamics and cell physiology. *Nat Rev Mol Cell Biol* 2:908–16

Supplementary Information accompanies the paper on the Journal of Cerebral Blood Flow & Metabolism website (http://www.nature.com/jcbfm)